RESEARCH Open Access



Evidence for reduced choroid plexus volume in the aged brain

R. Youh^{1†}, C. Perera^{1†}, C. Katsiva¹, I. F. Harrison¹, M. F. Lythgoe¹, D. K. Wright², S. Nizari¹ and Jack A. Wells^{1*}

Abstract

Background The choroid plexus plays an important role in brain homeostasis, including the active secretion of cerebrospinal fluid. Its function and structure have been reported to be affected by normal ageing. However, existing measures of choroid plexus volume may be complicated by partial volume (in vivo MRI) and tissue fixation artefacts (histology). In this study, we investigate possible changes in choroid plexus volume within the lateral ventricles of aged mice utilising two structural MRI protocols explicitly designed for time-efficient, high-resolution in vivo imaging of the choroid plexus.

Methods Two MRI sequences were utilised to examine in vivo choroid plexus volume in the lateral ventricles of young (\sim 6 months) and aged (\sim 24 months) mouse brains: (1) an ultra-long echo-time T2 weighted fast-spin-echo and (2) a multi-TE T2* mapping protocol. A test-retest study was performed on a subset of the data to examine the reproducibility of choroid plexus volume estimation based on manual segmentation. A two-way ANOVA test was performed to determine possible differences in choroid plexus volume in young and aged mouse groups across the two distinct MRI protocols.

Results Reproducibility tests showed a low test-retest variability of the manual segmentation pipeline for both MRI protocols. A statistically significant reduction of in vivo choroid plexus volume was found in the aged mouse brain. This finding is concordant with previous histological observations of a reduction in epithelial cell height with ageing across a wide range of species.

Conclusions We present an in vivo investigation of changes to lateral ventricle choroid plexus volume in the mouse brain utilising a manual segmentation approach based on two bespoke MRI protocols designed for time-efficient high resolution imaging of the choroid plexus. Based on these protocols, we provide evidence for a reduction in choroid plexus volume in the aged brain. This research provides insight for studies utilising MRI measurements of choroid plexus volume as a biomarker of age-related neurologic conditions as it indicates that the ageing process itself does not result in hypertrophy of the choroid plexus, but a decrease in tissue volume.

[†]R. Youh and C. Perera joint first authors.

*Correspondence: Jack A. Wells jack.wells@ucl.ac.uk

¹UCL Centre for Advanced Biomedical Imaging, Division of Medicine,

University College London, London, UK

²Department of Neuroscience, The School of Translational Medicine, Monash University, Melbourne, Australia



© The Author(s) 2025. **Open Access** This article is licensed under a Creative Commons Attribution 4.0 International License, which permits use, sharing, adaptation, distribution and reproduction in any medium or format, as long as you give appropriate credit to the original author(s) and the source, provide a link to the Creative Commons licence, and indicate if changes were made. The images or other third party material in this article are included in the article's Creative Commons licence, unless indicated otherwise in a credit line to the material. If material is not included in the article's Creative Commons licence and your intended use is not permitted by statutory regulation or exceeds the permitted use, you will need to obtain permission directly from the copyright holder. To view a copy of this licence, visit http://creativecommons.org/licenses/by/4.0/.

Youh et al. Fluids and Barriers of the CNS (2025) 22:97 Page 2 of 8

Introduction

The choroid plexus (ChP) resides in the lateral, third, and fourth ventricles of the brain and forms the blood-cerebrospinal fluid barrier (BCSFB). The ChP performs several key roles in service of normal brain function including the active secretion of cerebrospinal fluid (CSF) which may in turn support the efficacy of CSF-mediated brain-clearance mechanisms such as the glymphatic pathway [1, 2]. Given this multifaceted and unique physiology, the ChP has been proposed as a hitherto underexplored site of mechanistic significance in age-related conditions such as multiple sclerosis (MS) and Alzheimer's disease (AD) [3–6].

Towards the goal of developing novel imaging biomarkers of ChP derangement, there has been an emergence of publications reporting changes in ChP volume associated with disease, based on segmentation of high-resolution structural MRI scans [7-15]. One notable observation in the context of age-related neurodegenerative disease, are reports of increased lateral ventricle (LV) ChP volume in the aged human brain [16, 17]. Interestingly, this finding would appear to contradict direct histological assessment where ChP epithelial atrophy has been reported with age in both mice and rats as well as in the human brain [18–20]. These reports are further complicated by possible methodological limitations associated with both approaches such as partial volume effects exacerbated by the retrospective analysis of structural MRI scans that were not explicitly designed for reliable ChP segmentation as well as possible artefacts due to tissue fixation procedures required in histology. Thus, we aimed to help disambiguate the relationship between LV ChP volume and ageing by acquiring in vivo measurements of ChP volume using two bespoke time-efficient MRI protocols designed for high-resolution in vivo imaging of the ChP: (i) an ultra-long echo-time (TE) T2 weighted fast-spin echo (FSE) scan and (ii) a multi-TE T2* mapping protocol. We demonstrate that both MRI protocols provide measures of ChP volume with low test-retest manualsegmentation variability. We then apply both imaging protocols to aged and young-adult control mice for noninvasive, in vivo estimation of ChP volume. Doing so returns evidence for a reduction in ChP volume in the aged brain, suggesting that the ageing process results in a decreased volume of ChP tissue.

Methods

Animal preparation

All experiments were conducted in accordance with the European Commission Directive 86/609/EEC (European Convention for the Protection of Vertebrate Animals Used for Experimental and Other Scientific Purposes) and the United Kingdom's Home Office Animals (Scientific Procedures) Act (1986). Prior to data collection, mice

were acclimatized in an animal facility with a 12-hour light/12-hour dark cycle, and food and water were provided ad libitum.

Imaging was performed using a horizontal-bore 9.4T Bruker preclinical system (BioSpec 94/20 USR; Bruker) equipped with a 440-mT/m gradient set featuring outer and inner diameters of 205 mm and 116 mm, respectively (BioSpec B-GA 12S2). An 86-mm volume transit RF coil and a four-channel receiver-array coil, specifically designed for mouse brain imaging (Bruker), were used for data acquisition. Mice were anesthetized with a 2% isoflurane mixture (4:1 room air/O₂), adjusted to 1.5% to maintain a respiratory rate of approximately 150 bpm, which was continuously monitored using a pressure pad throughout the scan. The mouse's head was rigidly fixed using blunt ear bars. Core body temperature was measured with a rectal probe (SA Instruments, Stony Brook, NY) and kept at 37.0 \pm 0.5 °C, regulated by an adjustable water bath connected to a mouse heating pad (Bruker BioSpec; Bruker, Kontich, Belgium). MRI experiments were performed on male C57BL/6JRj mice at 6 and 24 months of age (Janvier labs) (n = 10 and n = 12 respectively). This corresponds to an age in human years of approximately 30 and 70 years respectively [21].

Data acquisition

In this study, two structural MRI protocols designed for high resolution/contrast imaging of mouse ChP were applied in separate scan sessions: (1) 3D FSE ultra-long TE readout with the following parameters: FOV = $19.6 \times 19.6 \times 3.6$ mm (centred around the LVs, see Fig. 1); matrix size = $196 \times 196 \times 36$; 0.1 mm isotropic resolution; echo train length = 64; effective TE = 176.2ms; TR = 5000ms; 1 average; acquisition time ~ 6.5 min; (2) 3D multi-TE gradient echo with the following parameters; FOV = $16 \times 19.25 \times 12$ mm; matrix size = $128 \times 154 \times 96$; TEs = 2.19, 5.25, 8.31, 11.37, 14.43, 17.49, 20.55, 23.61, 26.67, 29.73, 32.79, 35.85 ms; TR = 66ms; flip angle = 15° ;1 average; 0.125 mm isotropic resolution; acquisition time ~ 16 min.

Both imaging datasets were collected to estimate the volume of ChP. The raw MRI images of the 3D FSE h-T2w readout were directly utilised, while the 3D multi-TE GRE T2*w readout was then used to generate T2* map images for ChP volume estimation by fitting the data to a simple mono-exponential model using Matlab (Mathsworks, Massachusetts, USA).

ChP volume estimation

A manual segmentation pipeline was conducted for in vivo ChP volume estimation in young and aged mouse brains among all image datasets (Fig. 1). For each slice, the ChP was manually segmented based on visual inspection of the T2w images/ T2* maps. The segmentations

Youh et al. Fluids and Barriers of the CNS (2025) 22:97 Page 3 of 8

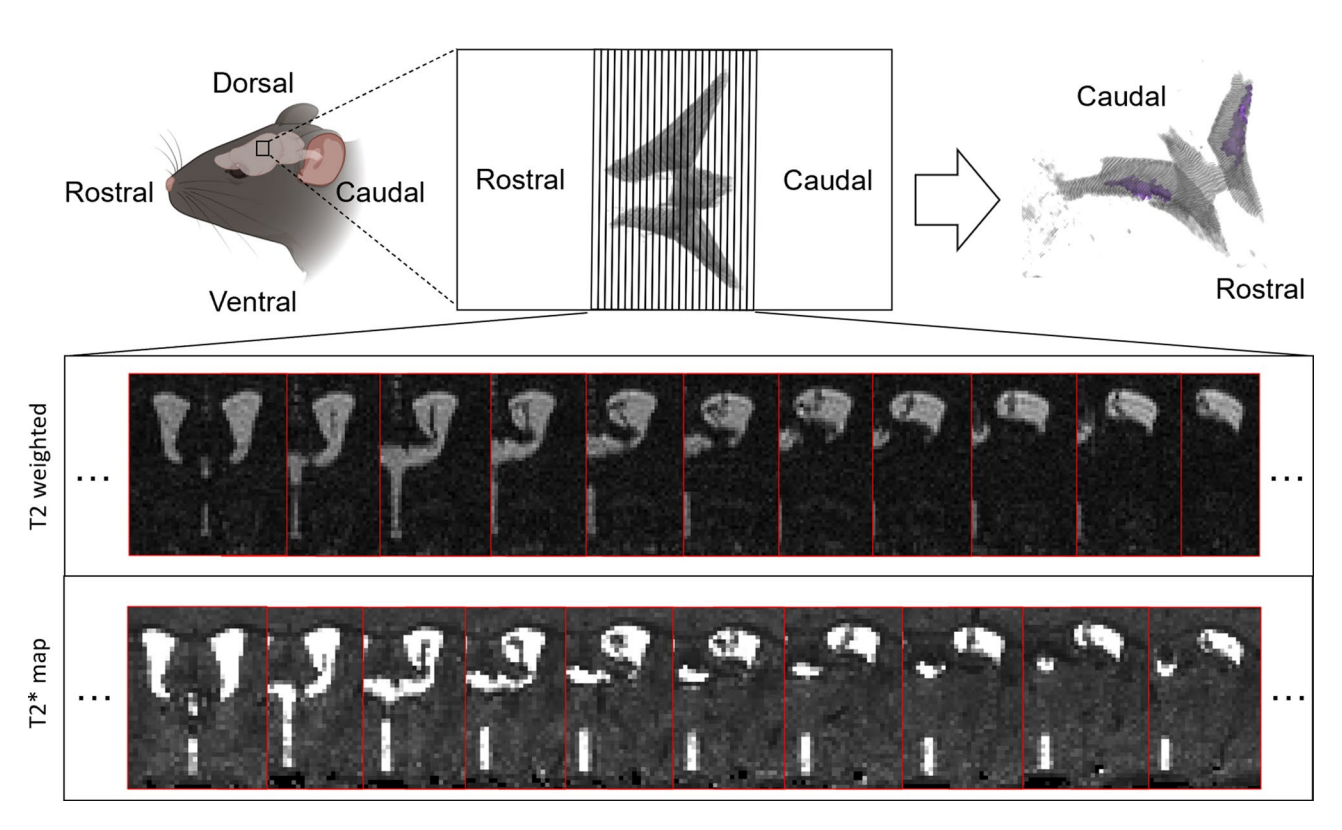


Fig. 1 Schematic of manual segmentation pipeline. Top: The LV images were extracted from the mouse brain (upper left and upper middle) using MRI protocols that are explicitly designed for ChP segmentation, where the ChP is viewed and manually segmented slice by slice (upper middle). The ChP (upper right) is then labelled within the LV and is highlighted in purple. Bottom: Representative datasets from the same subject utilising two different imaging protocols (T2w and T2* map, n=1 representative), which demonstrates a collection of sequential slices that capture the LV for ChP volume estimation

were carried out using the Volume Segmenter toolbox in MATLAB. The manual segmentation was performed blind to the animal group (aged vs. young control). To investigate the reproducibility of ChP volume estimation using the manual segmentation pipeline, the segmentation pipeline was repeated on 3 randomly selected subjects within a one-day interval. This was performed separately for both MRI protocols. The mean absolute % difference in volume measurements was calculated for each subject.

Statistical analysis

The effect of age and imaging protocol (ultra-long TE T2w & T2*maps) on ChP volume was investigated using a two-way analysis of variance (ANOVA) test using GraphPad Prism (GraphPad Software, Boston, Massachusetts USA). Errors are reported as standard deviations from the mean.

Results

ChP segmentation reproducibility test

Reproducibility tests were carried out to investigate the consistency of the manual ChP volume segmentation methods (Fig. 2). An average absolute change of 9.38% was observed between the repeatedly segmented datasets

using high-resolution ultra-long TE T2w MRI images (Fig. 2(A)), while an average absolute change of 7.07% was observed using T2* map images (Fig. 2(B)). A representative example of the reproducibility test is shown in Fig. 3(C)(D), where we observe a high degree of segmentation agreement for both protocols. Here, we established that the manual segmentation method yielded reproducible estimates of ChP volume.

In vivo choroid plexus volume in the aged mouse brain

A two-way ANOVA test was conducted to compare the main effects of age and MRI protocol as well as the interaction effects on the ChP volume. Prior to unblinding, one mouse was excluded from all T2* map analyses due to MRI artifacts within the LV that affected the segmentation. No other animals were excluded from the analysis. The age effect was statistically significant (P < 0.01). The effect of imaging datasets was statistically significant (P < 0.05). The interaction effects showed no significance (P > 0.05). A comparison of ChP volume between young (N = 10, $0.405 \pm 0.076 mm^3$) and aged mice $(N = 12, 0.356 \pm 0.036 \, mm^3)$ from long TE T2-weighted MRI images is shown in Fig. 3(A). A comparison of ChP volume between young $(N = 10, 0.481 \pm 0.129 \, mm^3)$ and aged mice $(N = 11, 0.129 \, mm^3)$

Youh et al. Fluids and Barriers of the CNS

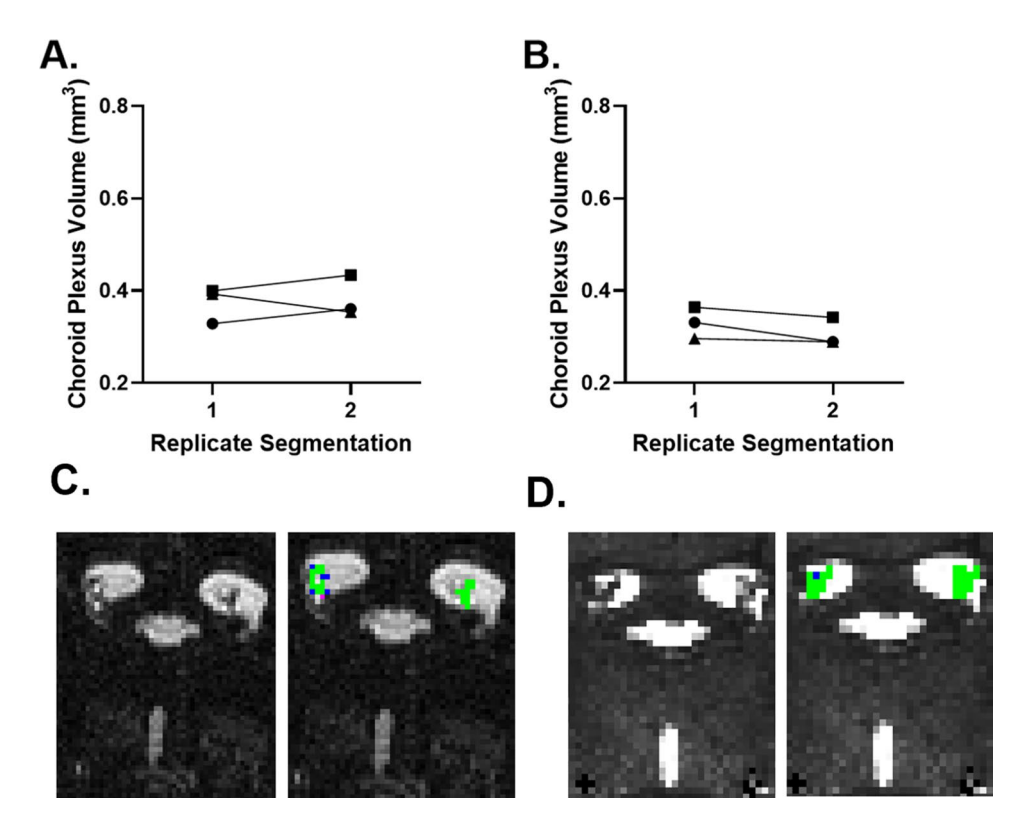


Fig. 2 Segmentation pipeline reproducibility tests. (**A**) ChP volume segmentation reproducibility test based on T2w datasets. (n = 3, randomly selected) (**B**) ChP volume segmentation reproducibility test based on T2* map datasets. (n = 3, randomly selected) (**C**) Representative example of visual comparison of sequential manual segmentation based on a T2w MRI image obtained from the reproducibility test. (**D**) Representative example of visual comparison of sequential manual segmentation based on a T2* map image obtained from the reproducibility test. For (**C**) and (**D**), the green areas indicate the regions segmented on both the first and second days. The purple areas represent the segmentations made on the first day that were not included on the second day. Conversely, the blue areas represent the segmentations made on the first day

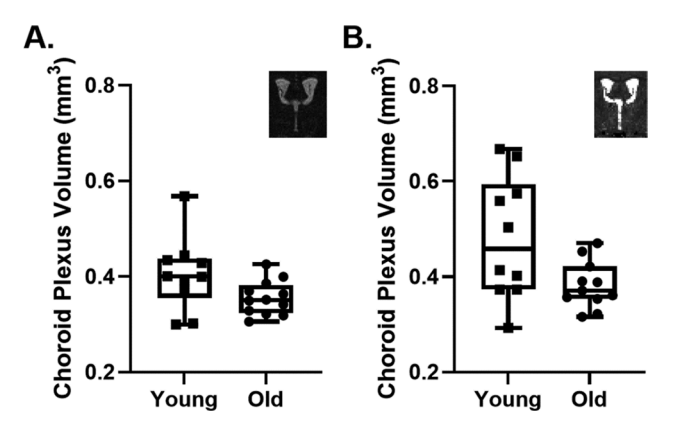


Fig. 3 Comparison of the ChP volume estimated in young and old groups from high-resolution T2-weighted MRI images (**A**) and T2* map MRI images (**B**). Each dot represents an individual mouse

 $0.383\pm0.050~mm^3$) from T2* map images is shown in Fig. 3(B). These findings indicate a statistically significant difference in ChP volume between the young and old groups.

Discussion

In this study we applied two time-efficient MRI protocols designed for robust estimation of ChP volume in the LVs of the mouse brain. The protocols employed were an ultra-long TE FSE and a multi-TE gradient echo T2* mapping sequence. We then evaluated the reproducibility of ChP volume estimates from manual segmentation of the images which returned a mean absolute difference of 9% and 7% for each protocol respectively, providing a solid foundation to detect putative group-wise differences in ChP volume in mouse models. We then applied the protocols to a cohort of aged and young mice to investigate possible changes in ChP volume in the ageing brain, given conflicting reports in the literature. Doing so, we found evidence for reduced ChP volume in the aged mouse brain, a finding concordant with observations of ChP epithelial atrophy from direct histological assessment [18-20]. This finding suggests that ageing causes atrophy of the ChP and highlights that this can be readily detected using non-invasive in vivo structural MRI. An important limitation of the current work is that the effect of age on ChP volume was investigated only in a single sex (male), thus limiting the relevance of our findings

[19]. Scarpetta and colleagues reported no differences due to sex in their recent histological characterisation of ChP changes in the aged mouse brain, suggesting that our observations are likely to extend to female mice. Future work, however, should be performed to characterise putative sex differences in structural alterations of the ChP with ageing.

It is important to note that some strains of mice such as BALB/c or DBA/2 have much smaller lateral ventricles in comparison to the C57BL/6 strain examined in this work [22]. This can make it challenging to accurately measure ChP volume using the protocols employed here. This is illustrated in Supplementary Fig. 1 where example images taken from a 5-week-old BALB/C mouse are compared against equivalent scans from the C57BL/6 strain. We were unable to identify ChP tissue on images acquired in the BALB/c strain despite confirming the presence of ChP tissue on histology (see Supplementary Fig. 1). Therefore, future studies should carefully consider the background strain of their mice when intending to apply non-invasive MRI protocols for in-vivo assessment of ChP volume.

The concept of the ultra-long FSE sequence for timeefficient imaging of ChP volume is a simple one that has been used before in MRI studies primarily designed to image the CSF [23, 24]. This employs a long echo train (in this case 64) which allows the acquisition of multiple lines of k-space after a single excitation for time-efficient data capture (in this case giving 0.1 mm isotropic resolution images in ~ 6 min). The resultant long echo time (TEeff = 176ms) will highly attenuate the signal from all tissue types within the brain with the exception of CSF due to its uniquely long T2 relaxation time ($\sim 300 \text{ms}$ [25]). Thus, in these images, negative contrast is employed where the CSF appears bright and the ChP tissue is dark. Accordingly, a downside of this approach is that all extra-ventricular tissue signal is nulled in these images meaning that this protocol will only inform about ventricular and ChP structure and not other grey/white matter regions for example. Here we implemented a 3D FSE sequence as image quality was found to be poor using an equivalent 2D sequence with matched geometry likely due to the cumulative effect of multiple refocusing pulses when using 0.1 mm slice thickness (data not shown). The multi-echo gradient echo 3D sequence is designed for time-efficient T2* mapping using a short TR and reduced flip angle. Similarly, this exploits the marked difference in T2* between the ChP and adjacent CSF. Unlike the ultra-long TE FSE sequence however, this also yields T2* maps across the extra-ventricular tissue which could be useful for detection of other radiological markers of pathology, such as micro-hemorrhages.

In regards to employing a more automated and objective approach to ChP volume estimation, within the

ultra-long TE FSE data we explored using signal-intensity based thresholding across the LVs under the premise that there would be two distinct signal populations at \sim 0 signal (ChP) and > >0 signal (CSF). However, the distribution of signal intensities within the LVs was found to more continuous and not as bi-modal as we initially surmised meaning that it was challenging to define a 'cutoff' signal intensity to accurately separate ChP and CSF voxels. We suspect that this principally reflects the partial volume of the CSF with tissue at the edge of the ventricles and ChP respectively, in addition to some subtle Gibbs ringing artefacts in the CSF (whose characteristic pattern can be distinguished by eye). Thus, we proceeded with a manual segmentation approach which further benefits from the experience of the rater to recognise the characteristic morphology of the ChP within the LVs (see Fig. 1). Indeed, this approach returned a mean absolute error in ChP volume estimation of 9% (ultra-long TE FSE) and 7% (multi-TE GE T2* maps) following test-retest ChP segmentations suggesting that this approach can yield reliable estimates of ChP volume. Moving forward, the use of more automated approaches may alleviate the need for the time-consuming manual segmentation [17, 26, 27]. Interestingly, the estimates of ChP volume based on the T2* maps were greater than those using the ultra-long TE FSE protocol which likely stems from a 'blurring' of the ChP tissue due to the macro time-invariant susceptibility effects that are present with T2* vs. T2 contrast.

Our finding of reduced ChP volume in the aged brain is consistent with histological observations of epithelial cell atrophy in the aged mouse, rat and human brain [18–20]. Although, it is important to point out that a recent study in rats found no evidence for ChP cell atrophy at 24 months of age [28]. The precise reasons why, based on in vivo structural MRI data, we find a reduction in ChP volume in the aged mouse brain whereas others have reported an increase in ChP volume with ageing in the human brain [16, 17], remains unknown at this time. Here, we speculate the following methodological/ physiological factors may be at play: (i) the limited spatial resolution of in vivo structural MRI scans to accurately spatially resolve the fine structure of the ChP may lead to systematic errors that influence the accuracy of ChP volume measurement. This may be impacted by changes in the volume of the LVs that occur with ageing, in turn altering the expanse of fluid in which the ChP tissue can float within. ChP tissue that is diffusely present in a larger volume of ventricular CSF could be misinterpreted as possessing a greater volume than ChP tissue more densely packed into a small volume of lateral ventricular CSF due to partial volume effects given the limited spatial resolution of the images. In the mice examined here, no significant differences in our in vivo measurements of ventricular volume were detected between the aged and young adult groups, as found in our previous study [29] (data not shown). It could also be related to the presence of ChP cysts that were recently captured with high resolution imaging of the human brain at 7T [30]. These cysts which would likely act to artificially enhance measures of ChP volume from in-vivo structural MRI scans, where the outer surface of the CP tissue is typically segmented to estimate it's volume. (ii) earlier studies have reported an increased volume of ChP tissue in a range of neurological conditions (e.g [11, 31-35]). Of note, to our knowledge a decrease in ChP volume associated with a disease has yet to be reported. Therefore, the increased ChP volume observed in the aged human brain may reflect undiagnosed comorbidities with human ageing that are not necessarily recapitulated in the aged mouse brain, highlighting the limitations of the mouse to model the complex multifaceted co-morbidities that come with human ageing. (iii) the ChP is known to undergo marked movement due to cardiac and respiratory pulsation. As, to our knowledge, none of the previous studies of ChP volume have been gated to cardiac or respiratory signals (including the present work), this movement may introduce a degree of inaccuracy into the structural images where ChP tissue that undergoes a greater degree of motion presents with a spurious increase in volume due to blurring during the acquisition (which typically takes several minutes). This possible artefact may have an age dependence where, in the case of cardiac pulsation, upstream stiffening of the vessels leads to greater pulse wave propagation to the downstream cerebral vessels [36]. Our preliminary investigation into the degree of ChP motion with cardiac and respiratory cycles suggested that this motion was subtle however and will thus have relatively little influence on our ChP volume measurements (data not shown).

To our knowledge, the weight of the mouse ChP has not been reported in the literature (and by extension the weight of the mouse brain ChP in the LVs). Interpolating the rat ChP weight of 2.9 mg [37, 38] and assuming that the weight/volume of the mouse brain is 20% of the rat brain, this gives an approximate weight of the mouse ChP of 0.58 mg. Based on prior measurements of the surface area of the ChP in the mouse brain [39] the ChP in the LVs represents 43% of the total ChP tissue giving an estimated mass of 0.25 mg. We estimate ChP volume to be 0.40 and 0.48 mm³ for our two MRI protocols in the young mouse brain. Therefore, assuming the ChP tissue has the density of water, there is an approximately two-fold overestimation in the volume of the ChP using our MRI protocol. This is perhaps not surprising as partial volume effects are notoriously challenging using non-invasive in-vivo imaging of the ChP, given it's fine and delicate structure which is microscopically intertwined with the CSF and often directly proximal to the ventricular wall. Nonetheless, this inaccuracy does not necessarily confound measures of differences in ChP volume between different groups (here young vs. old), but reinforces the need to carefully consider the imaging methods (spatial resolution/ contrast etc.) when comparing MRI-derived estimates of in-vivo ChP volume from different studies. In their recent examination of ChP morphology in the aged mouse brain, Scarpetta and colleagues found a $\sim 10\%$ and $\sim 30\%$ decrease in epithelial cell area and microvilli length when comparing 2 and 20 month old mice [19]. Similarly Serot et al., reported a 15% decrease in epithelial cell height when comparing 30 and 6 month old rats [18]. Here, we measure a 12% and 20% decrease in ChP volume with age for the ultra-long TE T2-weighted and T2* map scans respectively (when comparing mice at 6 and 24 months of age). Thus, the volume changes are broadly consistent with decreases in ChP cell dimensions previously reported.

Recently, studies have reported an association between ChP volume and neurological disorders such as AD, MS, and Parkinson's disease (PD). An earlier investigation found that an increased ChP volume is associated with patients with AD, as determined by T1-weighted (T1w) MRI scans [35]. This investigation also emphasised the need for more accurate measurement techniques to delineate ChP volume in MRI scans, alongside the development of effective segmentation methods [35]. In addition, a retrospective analysis indicated that the ChP volume within the LV is greater in individuals with Alzheimer's disease compared to those experiencing subjective cognitive impairment (SCI) or mild cognitive impairment (MCI), as assessed through 3D T1w imaging [15]. Apart from AD, a previous study has shown that patients with MS, particularly those with the relapsingremitting form, exhibit a larger ChP volume compared to healthy individuals based on 3D T1w images and that this enlargement is speculated to be partially related to inflammatory processes [40]. Another retrospective study reported ChP enlargement, based on T1w MRI images, may indicate a higher risk of developing dementia with PD [41]. Apart from studies related to neurological disorders, other human studies also reported an increase in ChP volume with normal ageing. For example, a cross-sectional study reported that larger ChP volume in the LVs was associated with older age. In addition, this cross-sectional study also emphasises the need for enhanced image resolution and improved segmentation techniques to more precisely evaluate ChP volume [16]. Another study developed a deep learning segmentation method to assess the ChP volume in the human brain utilizing T1w MRI, T2w MRI, and T2w FLAIR MRI images and reported a positive association between ChP volume and age in all three MRI protocols [17]. Further studies, including longitudinal studies and functional

investigations of ChP, are warranted to elucidate the complex interplay between ChP morphology, function, and ageing. In addition, preclinical studies including mouse models of AD, PD, MS, and other conditions, could utilise the MRI acquisition and analysis methods presented in this study. These approaches may enhance the understanding of the utility of MRI measurement of ChP volume as biomarkers of disease processes, with additional comparison with invasive assessment techniques.

To conclude, in this work we aimed to better understand the impact of ageing on ChP volume, captured using simple, translational, structural MRI scans. We did this by applying two MRI protocols specifically designed for efficient, high resolution, high contrast imaging of the ChP, to the young and aged mouse brain. We find evidence for a reduction in ChP volume in the aged brain, with both methods returning similar findings. This provides evidence that ageing itself results in atrophy and not hypertrophy of the ChP.

Supplementary Information

The online version contains supplementary material available at https://doi.org/10.1186/s12987-025-00716-y.

Supplementary Material 1

Acknowledgements

JAW, CP, CK and SN are supported by the Wellcome Trust (225345/Z/22/Z). IH is supported by a Parkinson's UK senior fellowship (SFEL-19-02), M.J.P. van Osch reports support from the Leducq Foundation and the Leducq Foundation for Cardiovascular Research (23CVD03), a NWO-Human Measurement Models 2.0 grant (18969) as well as support from the Dutch Research Council (NWO), European Community, the Dutch Heart Foundation, and the Dutch Brain Foundation. DLT is supported by the National Institute for Health and Care Research University College London Hospital Biomedical Research Centre (NIHR UCLH BRC), the Alzheimer's Society, and UK Research and Innovation (UKRI). LH is supported by an EU Joint programme-Neurodegenerative Disease Research (JPND) project (HCBI: "Human brain clearance imaging: a window on physiological disturbances in the prediagnostic phase of neurodegenerative diseases"). The project has received funding from the European Union's Horizon 2020 Research and Innovation Programme under grant agreement number 825664. Additional funding was received by Alzheimer Netherland (MJPvO, LH).

Author contributions

RY: Project lead, data analysis, data acquisition, Writing—original draft. CP: Supervision, data acquisition, Methodology, Writing—review and editing. CK: data analysis; IFH: Project Licence; Writing—review and editing. ML: Project licence, Writing—review and editing. DW: methodology, Writing—review and editing. SN: Supervision, data acquisition, Writing—review and editing. JW: Conceptualization, Resources, Formal analysis, Supervision, Funding acquisition, Investigation, Writing—review and editing, Project administration.

Funding

JAW, CP, CK and SN are supported by the Wellcome Trust (225345/Z/22/Z). DW is supported by the National Health and Medical Research Council to DKW [grant number: 1174040]. IFH is supported by both Parkinson's UK (F-1902) and Alzheimer's Research UK (ARUK-RF2019A-003). MFL is supported by Rosetrees Trust and the John Black Charitable Foundation (Grant No. A2200); Medical Research Council (MR/M009092/1); the Brain Tumour Charity (Grant No. QfC_2018_10387); the Edinburgh-UCL CRUK Brain Tumour Centre of Excellence (Grant No. C7893/A27590);

the CRUK & EPSRC Comprehensive Cancer Imaging Centre at KCL and UCL (Grant No. C1519/A16463 and C1519/A10331).

Data availability

Upon publication, the MRI data will be made freely available to download from the UCL data repository (https://rdr.ucl.ac.uk/authors/Jack_Wells/6768476).

Declarations

Ethics approval and consent to participate

All experiments were conducted in accordance with the European Commission Directive 86/609/EEC (European Convention for the Protection of Vertebrate Animals Used for Experimental and Other Scientific Purposes) and the United Kingdom's Home Office Animals (Scientific Procedures) Act (1986).

Competing interests

The authors declare no competing interests.

Received: 12 March 2025 / Accepted: 26 September 2025 Published online: 07 October 2025

References

- Courtney Y, Hochstetler A, Lehtinen MK. Choroid plexus pathophysiology. Annu Rev Pathol. 2024.
- MacAulay N, Keep RF, Zeuthen T. Cerebrospinal fluid production by the choroid plexus: a century of barrier research revisited. Fluids Barriers CNS. 2022:19(1):26
- Jiang J, et al. Choroid plexus volume as a novel candidate neuroimaging marker of the alzheimer's continuum. Alzheimers Res Ther. 2024;16(1):149.
- 4. Čarna M, et al. Pathogenesis of alzheimer's disease: involvement of the choroid plexus. Alzheimers Dement. 2023;19(8):3537–54.
- Magliozzi R, et al. Neuropathological and cerebrospinal fluid correlates of choroid plexus inflammation in progressive multiple sclerosis. Brain Pathol. 2024;e13322
- Hochstetler A, Lehtinen MK. Choroid plexus as a mediator of CNS inflammation in multiple sclerosis. Mult Scler. 2024:13524585241292974.
- Sun Z, et al. Choroid plexus aging: structural and vascular insights from the HCP-aging dataset. Fluids Barriers CNS. 2024;21(1):98.
- Li J, et al. Associations between the choroid plexus and Tau in alzheimer's disease using an active learning segmentation pipeline. Fluids Barriers CNS. 2024;21(1):56.
- Pearson MJ, Wagstaff R, Williams RJ. Choroid plexus volumes and auditory verbal learning scores are associated with conversion from mild cognitive impairment to alzheimer's disease. Brain Behav. 2024;14(7):e3611.
- Dai T, et al. Choroid plexus enlargement in amyotrophic lateral sclerosis patients and its correlation with clinical disability and blood-CSF barrier permeability. Fluids Barriers CNS. 2024;21(1):36.
- 11. Jeong SH, et al. Choroid Plexus Volume, Amyloid Burden, and Cognition in the Alzheimer's Disease Continuum. Aging Dis; 2024.
- 12. Umemura Y, et al. Choroid plexus enlargement in mild cognitive impairment on MRI: a large cohort study. Eur Radiol. 2024;34(8):5297–304.
- Assogna M, et al. Association of choroid plexus volume with serum Biomarkers, clinical Features, and disease severity in patients with frontotemporal Lobar degeneration spectrum. Neurology. 2023;101(12):e1218–30.
- Novakova Martinkova J, et al. Longitudinal progression of choroid plexus enlargement is associated with female sex, cognitive decline and ApoE E4 homozygote status. Front Psychiatry. 2023;14:1039239.
- Choi JD, et al. Choroid plexus volume and permeability at brain MRI within the alzheimer disease clinical spectrum. Radiology. 2022;304(3):635–45.
- Alisch JSR, et al. Characterization of Age-Related differences in the human choroid plexus Volume, microstructural Integrity, and blood perfusion using multiparameter magnetic resonance imaging. Front Aging Neurosci. 2021;13:734992.
- 17. Eisma JJ, et al. Deep learning segmentation of the choroid plexus from structural magnetic resonance imaging (MRI): validation and normative ranges across the adult lifespan. Fluids Barriers CNS. 2024;21(1):21.
- Serot JM, et al. Choroid plexus and ageing in rats: a morphometric and ultrastructural study. Eur J Neurosci. 2001;14(5):794–8.

- Scarpetta V, et al. Morphological and mitochondrial changes in murine choroid plexus epithelial cells during healthy aging. Fluids Barriers CNS. 2023;20(1):19.
- Serot JM, et al. Morphological alterations of the choroid plexus in late-onset alzheimer's disease. Acta Neuropathol. 2000;99(2):105–8.
- Flurkey CH, D E, American College of Laboratory Animal Medicine Series.
 2007
- Hino K, et al. Strain differences of cerebral ventricles in mice: can the MRL/ MpJ mouse be a model for hydrocephalus? Jpn J Vet Res. 2009;57(1):3–11.
- Harrison IF, et al. Non-invasive imaging of CSF-mediated brain clearance pathways via assessment of perivascular fluid movement with diffusion tensor MRI. Elife. 2018:7.
- 24. Petitclerc L, et al. Ultra-long-TE arterial spin labeling reveals rapid and brain-wide blood-to-CSF water transport in humans. NeuroImage. 2021:245:118755.
- Lee H, et al. Choroid plexus tissue perfusion and blood to CSF barrier function in rats measured with continuous arterial spin labeling. NeuroImage. 2022;261:119512.
- Yazdan-Panah A, et al. Automatic segmentation of the choroid plexuses: method and validation in controls and patients with multiple sclerosis. Neuroimage Clin. 2023;38:103368.
- Storelli L, et al. A fully automatic method to segment choroid plexuses in multiple sclerosis using conventional MRI sequences. J Magn Reson Imaging. 2024;59(5):1643–52.
- Lolansen SD, et al. Choroid plexus-mediated CSF secretion remains stable in aging rats via high and age-resistant metabolic activity. Nat Commun. 2025;16(1):6778.
- Evans PG, et al. Non-invasive MRI of blood-cerebrospinal fluid barrier function. Nat Commun. 2020;11(1):2081.
- Zhen Z, et al. Choroid plexus cysts on 7T MRI: relationship to aging and neurodegenerative diseases. Alzheimers Dement. 2025;21(2):e14484.
- Sun S, et al. Elevated peripheral inflammation is associated with choroid plexus enlargement in independent sporadic amyotrophic lateral sclerosis cohorts. Fluids Barriers CNS. 2024;21(1):83.

- 32. Kolahi S, et al. Choroid plexus volume changes in multiple sclerosis: insights from a systematic review and meta-analysis of magnetic resonance imaging studies. Neuroradiology. 2024;66(11):1869–86.
- 33. de Deus Vieira G, Antônio FF, Damasceno A. Enlargement of the choroid plexus in pediatric multiple sclerosis. Neuroradiology. 2024;66(7):1199–202.
- 34. Ota M, et al. Relationship between the Tau protein and choroid plexus volume in alzheimer's disease. NeuroReport. 2023;34(11):546–50.
- Tadayon E, et al. Choroid plexus volume is associated with levels of CSF proteins: relevance for alzheimer's and parkinson's disease. Neurobiol Aging. 2020:89:108–17.
- Aquaro GD, et al. Age-dependent changes in elastic properties of thoracic aorta evaluated by magnetic resonance in normal subjects. Interact Cardiovasc Thorac Surg. 2013;17(4):674–9.
- 37. Keep RF, Jones HC. A morphometric study on the development of the lateral ventricle choroid plexus, choroid plexus capillaries and ventricular ependyma in the rat. Brain Res Dev Brain Res. 1990;56(1):47–53.
- Quay WB. Regional and quantitative differences in the postweaning development of choroid plexuses in the rat brain. Brain Res. 1972;36(1):37–45.
- Knudsen PA. THE SURFACE AREA OF CHOROID PLEXUS IN NORMAL MOUSE EMBRYOS. Acta Anat (Basel). 1964;58:355–64.
- Ricigliano VAG, et al. Choroid plexus enlargement in inflammatory multiple sclerosis: 3.0-T MRI and translocator protein PET evaluation. Radiology. 2021;301(1):166–77.
- 41. Jeong SH, et al. Association between choroid plexus volume and cognition in Parkinson disease. Eur J Neurol. 2023;30(10):3114–23.

Publisher's note

Springer Nature remains neutral with regard to jurisdictional claims in published maps and institutional affiliations.